arXiv:2601.16981v2 [cs.CV] 14 May 2026

SyncLight: Single-Edit Multi-View Relighting

David Serrano-Lozano
Computer Vision Center
Universitat Autònoma de Barcelona

Anand Bhattad†
Johns Hopkins University

Luis Herranz
Universidad Politécnica de Madrid

Jean-François Lalonde†
Université Laval

Javier Vazquez-Corral†
Computer Vision Center
Universitat Autònoma de Barcelona

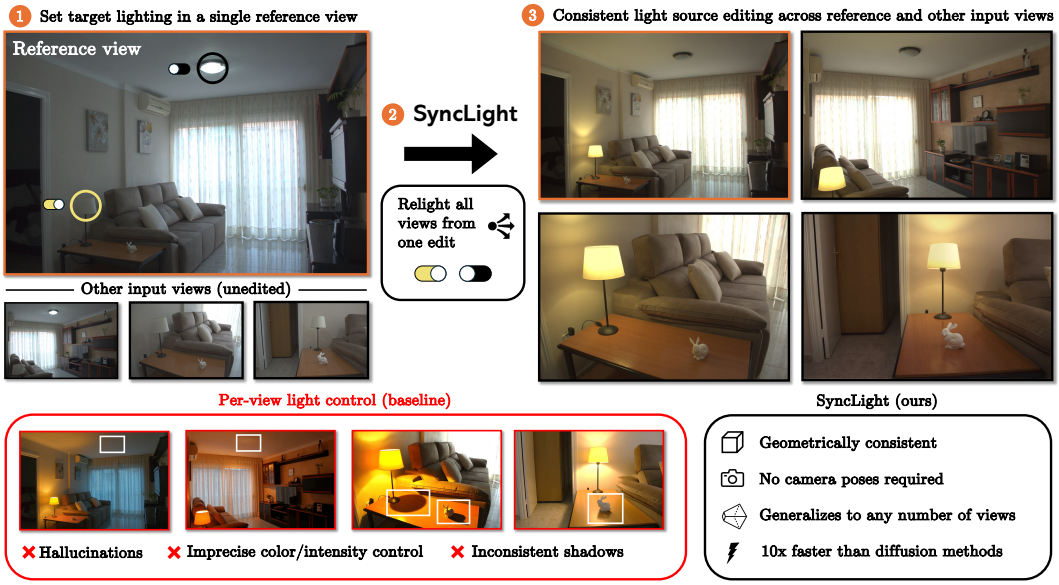


Figure 1: Multi-view light editing with SyncLight. Given an uncalibrated, multi-view capture of a static scene (1), the user selects one frame as the *reference view* and specifies the desired lighting by clicking on one or many visible light sources (circle markers), and setting their desired intensity and chromaticity. SyncLight (2) then relights all input views consistently, including the reference view itself (3). By leveraging a latent bridge matching formulation, SyncLight performs a *single* feedforward pass simultaneously across all views, and generalizes to an arbitrary number of viewpoints. Baseline per-view light control methods (bottom-left) fail to produce coherent results, suffering from hallucinations, imprecise control, and inconsistencies across views. In contrast, SyncLight is geometrically consistent, requires no camera poses, generalizes to any number of views, and is 10× faster than current diffusion and flow-matching models.

Abstract

We present **SyncLight**, a method to enable consistent, parametric control over light sources across multiple uncalibrated views of a static scene conditioned on a single view. While single-view relighting has advanced significantly, existing generative approaches struggle to maintain the rigorous lighting consistency essential for multi-camera broadcasts, stereoscopic cinema, and virtual production. SyncLight addresses this by enabling precise control over light intensity and color across a multi-view capture of a scene, conditioned on a single reference edit. Our method leverages a multi-view diffusion transformer trained using a latent bridge matching

†indicates equal advising. Project Page: `https://sync-light.github.io/`

formulation, achieving high-fidelity relighting of the entire image set in a single inference step. To facilitate training, we introduce a large-scale hybrid dataset comprising diverse synthetic environments—curated from existing sources and newly designed scenes—alongside high-fidelity, real-world multi-view captures under calibrated illumination. Though trained only on image pairs, SyncLight generalizes zero-shot to an arbitrary number of viewpoints, effectively propagating lighting changes across all views, without requiring camera pose information. SyncLight enables practical relighting workflows for multi-view capture systems. Dataset, code, and models will be released upon acceptance.

1 Introduction

Controlling illumination after capture in multi-view settings remains an open problem, even as neural rendering [47, 29] has made high-fidelity 3D geometry capture increasingly accessible. This is especially difficult for indoor scenes, where multiple light sources, interreflections, and occlusions create a rich illumination landscape—and where professional workflows like stereoscopic cinema and virtual production demand rigorous consistency, not just plausible appearance.

Relighting is fundamentally an ill-posed problem: from captured images alone, one cannot uniquely decompose appearance into geometry, material, and lighting. State-of-the-art generative methods like LightLab [45] and ScribbleLight [10] achieve photorealistic single-image editing, but process each view independently and hallucinate lighting effects that are locally plausible yet globally contradictory: shadows change direction between cameras, specular highlights remain stationary as viewpoints shift. Conversely, inverse rendering and NeRF-based approaches [67, 24] enforce physical consistency through explicit geometry estimation, but require known camera poses, expensive per-scene optimization, and struggle in regions where geometric estimates fail.

To resolve this dichotomy, we introduce **SyncLight**, a *pose-free* generative framework that brings the flexibility of 2D image editing to multi-view indoor scene relighting. Unlike prior multi-view approaches that depend on calibrated cameras or explicit 3D reconstruction, SyncLight operates directly on uncalibrated image sets: a multi-view diffusion transformer learns to discover cross-view correspondences implicitly through attention, sidestepping both the ill-posed decomposition and the brittle reliance on geometric supervision. A user adjusts light intensity and color on a single reference image, and SyncLight propagates these changes across all synchronized viewpoints in a single forward pass, preserving the complex interplay of shadows, highlights, and indirect illumination.

Realizing this system requires addressing two challenges. First, no existing dataset provides multi-view captures with calibrated lighting ground truth; we introduce a large hybrid dataset combining procedurally generated synthetic environments with high-fidelity real-world captures. Second, prior video-based approaches require per-frame lighting specification, making editing tedious; our multi-view transformer instead propagates a single reference edit jointly to all views, again without any pose information. A key emergent property is *zero-shot scalability*: although trained exclusively on image pairs ($N = 2$), our attention mechanism generalizes to dense camera arrays ($N > 2$) at inference without retraining. Fig. 1 illustrates this workflow, where users click on the reference image to control intensity and chromaticity, and the edits propagate consistently across all views.

In summary, we make the following contributions:

- **Pose-free multi-view relighting:** The first generative method to parametrically relight synchronized, uncalibrated views with strict spatial and photometric consistency in a single forward pass—without any camera poses or explicit 3D reconstruction.
- **Zero-shot generalization:** A relighting-aware Multi-View Transformer that learns consistency from image pairs while scaling to arbitrary view counts at inference.
- **Efficient one-step inference:** Bridge matching delivers high-fidelity results in a single pass, providing a production-ready alternative to slow optimization baselines.
- **SyncLight dataset:** A comprehensive dataset of multi-view indoor scenes under varying illumination, bridging synthetic and real-world domains.

2 Related Work

The paradigm of relighting has recently shifted from physically-based inverse rendering [34, 33, 62, 36, 68, 25, 26, 17, 16, 35] to data-driven generative modeling. Rather than explicitly solving the ill-posed decomposition of appearance into geometry, materials, and lighting, modern approaches learn to hallucinate plausible lighting transformations directly in image space [7, 65, 57, 45], leveraging the fact that such decompositions can emerge implicitly within generative models [6, 12].

Domain-specific methods. Early generative approaches focused on constrained settings. Portrait relighting methods leverage light stage captures [20, 46] to model facial appearance under controlled illumination, but are limited to frontal faces. Object-centric approaches [60, 11, 23, 5, 66, 15, 3] condition diffusion models on environment or intrinsic maps, spherical harmonics, or shadow masks, enabling material-aware relighting for isolated objects. However, these methods do not generalize well to complex indoor scenes with multiple interacting light sources and global illumination.

Single-view diffusion for general indoor scenes. Recent diffusion-based methods achieve remarkably photorealism by framing relighting as conditional synthesis. IC-Light [63] leverages large 2D datasets to hallucinate lighting effects based on text or environment maps, while LumiNet [57] and StyLitGAN [7] explore unsupervised latent control [65] but suffer from intrinsic ambiguities. Methods such as IntrinsicEdit [44], IID [31], LightIt [30], PractiLight [13], and RGB$\leftrightarrow$X [61] use intrinsic representations for relighting, though they require explicit maps or lack spatial control.

ScribbleLight [10] and LightLab [45] are state-of-the-art in single-view relighting. Both process views independently and cannot maintain cross-camera consistency. SyncLight instead uses cross-view attention to propagate a single reference edit across all views in a single forward pass, requiring no per-view masks, depth, or camera poses. Trained only on stereo pairs, it generalizes zero-shot to larger camera arrays at inference. We further replace iterative diffusion (50+ steps) with Latent Bridge Matching for one-step inference (10–50$\times$ speedup).

3D-consistent approaches. NeRF- or 3DGS-based methods [67, 24, 3, 50, 41] and inverse rendering approaches enforce consistency through explicit 3D decomposition into geometry, materials, and lighting. While these ensure geometric consistency, they require per-scene optimization and lack flexibility for rapid editing. More recently, [8, 39] combine monocular geometry estimation with physically-based rendering to enable CG-like control over light placement in scenes. While this achieves physical accuracy, it requires explicit mesh reconstruction and does not address multi-view consistency constraints of synchronized camera arrays. SyncLight instead learns consistency priors directly from multi-view data using a generative prior without per-scene 3D reconstruction.

Multi-view generation and consistency. Recent work has shown that explicit cross-view attention is effective for enforcing geometric consistency. MVDream [53] introduced multi-view diffusion transformers for text-to-3D generation, demonstrating that shared attention across views yields consistent outputs. We build on this insight for relighting, showing that multi-view transformers trained on stereo pairs generalize zero-shot to larger camera arrays and wide-baseline stereo images never seen during training. Temporal consistency in video—conceptually analogous to spatial cross-view consistency—has been studied in recent video relighting work. RelightVid [14] and UniRelight [19] mitigate flickering via temporal modeling and joint denoising. However, these methods operate on sequential frames and do not enforce rigid geometric consistency across viewpoints.

Concurrent works such as LuxRemix [38] and GR3EN [58] also tackle multi-view indoor relighting, but differ considerably from our approach. LuxRemix performs per-view generative OLAT *decomposition* and harmonizes the decomposed lights into a relightable 3DGS representation. GR3EN instead requires *posed* multi-view inputs, reconstructs a radiance field, and distills a video-to-video relighting diffusion model back into the 3D model. Both therefore, rely on an explicit per-scene 3D reconstruction, and GR3EN additionally requires known camera poses. SyncLight, in contrast, is pose-free and purely 2D: cross-view consistency emerges from our multi-view transformer, and the entire image set is relit in a single feedforward pass without any per-scene optimization.

Flow matching and efficient sampling. Our use of Latent Bridge Matching [9] builds on recent advances in flow-based generative models. Flow Matching [40] introduced simulation-free training of continuous normalizing flows, enabling faster sampling than standard diffusion. Bridge Matching and Schrödinger Bridge methods [2, 54] further refine these approaches by optimizing transport between

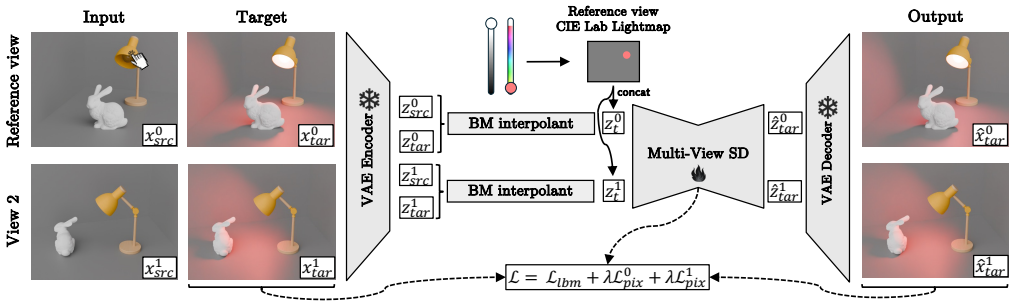


Figure 2: SyncLight formulates multi-view relighting as a conditional flow matching problem in latent space. (Left) Input scenes under source ($\mathbf{x}_{\text{src}}$) and target lighting ground truth ($\mathbf{x}_{\text{tar}}$) are encoded into latents ($\mathbf{z}_{\text{src}}, \mathbf{z}_{\text{tar}}$) via a VAE encoder. This is done for both the "Reference" (0) and "Other" (1) views. (Middle) During training, we sample a timestep t and construct a Bridge Matching (BM) interpolant $\mathbf{z}_t$. Our backbone, "Multi-View SD", is conditioned on a user-specified "Lightmap" (encoding color as intensity and chromaticity) derived from the "Reference view". To enforce consistency, the backbone processes both views simultaneously. (Right) The model predicts the target latents, which are decoded into relit images ($\hat{\mathbf{x}}_T$). The network is optimized using a hybrid objective $\mathcal{L}$ combining latent flow matching loss ($\mathcal{L}_{\text{lbm}}$) with pixel-level reconstruction losses ($\mathcal{L}_{\text{pix}}$) for each view to ensure high-fidelity, consistent relighting.

arbitrary distributions by adding stochasticity in the trajectory. We adopt this formulation to enable one-step inference essential for interactive multi-camera relighting workflows.

3 Method

Our goal is to enable consistent, parametric light-source control across multiple synchronized views by conditioning on parametric lighting edits applied to a single reference view. Unlike prior multi-view diffusion frameworks such as MVDream [53] or Wonder3D [43], which target image-to-3D generation and require explicit camera pose information, SyncLight is a pose-free, generative framework for editing light sources in synchronized views of an existing scene. Our model implicitly discovers cross-view correspondences through attention, without any geometric supervision, by specifying only the desired light conditions in one reference view. We build upon latent diffusion models [52] and extend them to the multi-view setting through two key contributions: (1) a multi-view transformer with cross-view attention that enforces spatial coherence and consistent propagation of lighting edits, and (2) LBM formulation [9] that enables one-step inference, avoiding the iterative sampling required by standard diffusion models. Fig. 2 provides an overview of our approach.

Latent bridge matching. Traditional latent diffusion models learn to denoise from pure Gaussian noise, which is inefficient for image-to-image translation tasks, where the source image already contains most of the desired scene content. Flow matching [40] provides a framework for learning continuous transport between arbitrary distributions. We adopt LBM [9], which constructs flows between a source latent $\mathbf{z}_{src}$ (encoding an image under source lighting) and a target latent $\mathbf{z}_{tar}$ (encoding the same scene under target lighting).

We encode an image under source and target lighting $\{\mathbf{x}_{\text{src}}, \mathbf{x}_{\text{tar}}\}$ into latent representations using a pretrained VAE encoder, $\mathbf{z} = \mathcal{E}(\mathbf{x})$, and define a stochastic interpolation path between them:

$$\mathbf{z}_t = (1-t)\mathbf{z}_{\text{src}} + t\mathbf{z}_{\text{tar}} + \sigma\sqrt{t(1-t)}\boldsymbol{\epsilon}\,, \tag{1}$$

where $t \in [0,1]$, $\boldsymbol{\epsilon} \sim \mathcal{N}(0, I)$, and σ controls the noise magnitude. Following prior work [42, 9, 55], we use $\sigma = 0.005$, resulting in stochastic trajectories.

The model $\mathbf{v}_\theta$ is trained to predict the velocity field that transports $\mathbf{z}_{\text{src}}$ to $\mathbf{z}_{\text{tar}}$. The target velocity is:

$$\mathbf{v} = \mathbf{z}_{\text{tar}} - \mathbf{z}_{\text{src}}. \tag{2}$$

The training objective minimizes the mean squared error between predicted and target velocities:

$$\mathcal{L}_{\text{lbm}} = \mathbb{E}_{t,\mathbf{z}_{\text{src}},\mathbf{z}_{\text{tar}}}\left[\left|\left|\frac{\mathbf{v}_\theta(\mathbf{z}_t, t, c)}{(1-t)} - \mathbf{v}\right|\right|_2^2\right], \tag{3}$$

where c is the conditioning information. We limit t to only 4 equally-spaced timesteps during training.

At inference time, given a source latent $\mathbf{z}_{\text{src}}$ and a conditioning c, the target latent is directly estimated in a *single* step. The decoded output $\hat{\mathbf{x}}_{tar} = \mathcal{D}(\hat{\mathbf{z}}_{tar})$ provides the relit image. Compared to iterative diffusion sampling (50+ steps), this one-step inference is significantly faster while maintaining high visual quality, making it practical for interactive multi-view applications. Observe that at $t = 0$, eq. (3) collapses to an L_2 loss between $\mathbf{v}_\theta$ and the residual $\mathbf{v}$, which might suggest that the LBM formulation reduces to standard regression under one-step inference. However, this is not the case: training across equally-spaced timesteps t forces the network to learn a well-conditioned velocity field along the entire stochastic interpolant, rather than a brittle point-to-point mapping; in line with the observations of [40], this multi-timestep supervision yields more generalizable transport even when inference is truncated to a single step. See Supplementary Material for further discussion.

Multi-view latent bridge matching. SyncLight takes as input two synchronized, uncalibrated views under source lighting $\{\mathbf{x}^0_{\text{src}}, \mathbf{x}^1_{\text{src}}\}$ and a lighting condition c^0 defined on the reference view $\mathbf{x}^0_{\text{src}}$, and predicts both views under target lighting $\{\hat{\mathbf{x}}^0_{\text{tar}}, \hat{\mathbf{x}}^1_{\text{tar}}\}$. Standard diffusion- or flow-based architectures are designed for single-image inputs and do not model cross-view interactions. We therefore use Stable Diffusion XL [49] as our velocity field model and adapt it to explicitly reason across multiple views while using its pretrained weights as the model initialization.

Inspired by MVDream [53], we replace each transformer block in SDXL with a multi-view transformer block. The key idea is to enable information exchange across N different views through modified self-attention. Given a batch of N view latents, we first process each view's features independently through the initial convolution layers. Before each transformer block, features from all views are concatenated along the token dimension rather than the batch dimension. This allows the self-attention mechanism to attend across views, capturing cross-view geometric and photometric consistency. After attention, features are reshaped back to the original per-view layout. Although we train exclusively on pairs ($N = 2$), the architecture is agnostic to the number of views due to the token-level attention mechanism. At inference, we observe generalization to arbitrary view counts while maintaining consistency (see sec. 5). Formally, the input to the model $\mathbf{v}_\theta$ is the batch-wise concatenation of all interpolated latent views: $\mathbf{z}_t = \text{concat}[\mathbf{z}^0_t, \cdots, \mathbf{z}^{N-1}_t]$. Despite this architectural inspiration, we note that our setting differs fundamentally: MVDream and related works (e.g., Wonder3D [43]) are image-to-3D *generative* models that require camera pose conditioning, whereas SyncLight is a pose-free parametric light source *editing* model operating on synchronous views.

Lighting control. We represent target lighting conditions via a 4-channel lightmap $L \in [-1, 1]^{H\times W\times 4}$ defined on the reference view $\mathbf{x}^0_{\text{src}}$. The only constraint on the reference view is that the light sources to be edited must be visible. Users specify locations of light sources to modify (via circular markers), and the lightmap encodes: (1) activation state (1 = on, -1 = off), and (2–4) target color in Lab space. All values default to 0, unless the user specifies the activation and color. We use Lab rather than RGB to enable independent control of brightness (L) and chromaticity (ab). The lightmap is resized to latent resolution and concatenated to each interpolated latent $\mathbf{z}^i_t$, yielding 8-channel inputs (4 latent + 4 lightmap). Since the pretrained SDXL backbone expects 4-channel latent inputs, we replace its first convolutional layer with an 8-channel variant whose four additional input channels (corresponding to the lightmap) are zero-initialized. Since all latents must have the same dimensions, we apply the same lightmap to all views—this works well in practice, likely because providing color and intensity hints to other views is helpful, even despite the spatial misalignment.

Training objective. In addition to the velocity-matching objective ($\mathcal{L}_{\text{lbm}}$ in eq. (3)), we follow prior work [9, 59] and impose reconstruction losses on the decoded images:

$$\mathcal{L} = \mathcal{L}_{\text{lbm}} + \lambda\mathcal{L}^0_{\text{pix}} + \lambda\mathcal{L}^1_{\text{pix}}\,, \tag{4}$$

where $\mathcal{L}^i_{\text{pix}}$ denotes the LPIPS loss [64] for view i. This perceptual LPIPS penalizes the blur-averaging failure mode, encouraging the network to produce confident, crisp predictions of shadow boundaries.

4 Dataset

Training a generative model for consistent multi-view relighting requires data satisfying three strict criteria: (1) diverse, high-fidelity indoor geometry; (2) perfectly synchronized multi-view camera poses; and (3) isolated, controllable light sources for supervision. Existing datasets fail to meet these requirements. To address this gap, we introduce the **SyncLight Dataset**, comprising nearly

Table 1: Quantitative multi-view image relighting results on our SyncLight test set. Each section of the table indicates which view is used to compute metrics: the "Reference (Ref.) view" (where edits are specified), "Second (Sec.) view" (another view in the set), and "Additional (Add.) views" (all but the reference view). Best results, achieved by SyncLight in all cases, are highlighted. See text for details on baselines. As SyncLight is always run on more than one image; no inference time is reported for the "Ref. view."

		Infinigen				BlenderKit				Real captures				
	Method	PSNR	SSIM	ΔE_{00}	LPIPS	PSNR	SSIM	ΔE_{00}	LPIPS	PSNR	SSIM	ΔE_{00}	LPIPS	Inf. time (s)
Ref. view	ScribbleLight	10.89	.518	30.67	.382	11.02	.528	29.26	.372	11.78	.483	28.36	.375	58.2 ± 1.14
	Flux.2-dev	14.23	.672	20.31	.338	16.71	.704	17.22	.291	18.32	.757	14.28	.264	55.6 ± 1.02
	LightLab*	29.86	.941	3.08	.131	26.38	.907	4.92	.147	28.42	.880	4.61	.199	1.17 ± 0.02
	SyncLight	31.32	.950	2.47	.119	27.16	.915	4.02	.134	30.34	.895	3.73	.196	-
Sec. view	Scribble+LNet	13.41	.498	19.67	.284	12.72	.507	23.91	.306	14.48	.518	23.77	.318	69.6 ± 1.82
	Flux.2-dev	12.75	.617	25.82	.386	14.92	.604	20.40	.469	16.35	.685	19.13	.305	111 ± 2.08
	LightLab*+LNet	17.36	.817	7.89	.184	15.92	.863	9.82	.196	20.46	.815	8.46	.279	13.1 ± 0.68
	SyncLight	31.45	.949	2.45	.119	28.19	.925	3.72	.126	30.23	.897	3.56	.197	1.58 ± 0.02
Add. views	Scribble+LNet	13.36	.494	19.65	.292	12.88	.509	23.47	.299	14.29	.525	23.92	.320	89.7 ± 1.93
	Flux.2-dev	12.55	.616	26.03	.388	14.90	.606	20.03	.472	16.21	.678	20.42	.328	273 ± 3.87
	LightLab*+LNet	17.22	.808	8.35	.195	16.07	.871	10.43	.185	20.40	.809	8.93	.287	38.5 ± 0.83
	SyncLight	31.42	.941	2.57	.122	28.01	.929	3.78	.125	30.44	.905	3.57	.194	2.38 ± 0.03

one million multi-view image pairs under diverse lighting conditions, designed to enable learning of physically consistent relighting across viewpoints.

Following prior work [22, 1, 45, 21], we employ a One Light At a Time (OLAT) capture scheme: for each scene, we render or photograph each controllable light source independently, together with an ambient capture containing only non-controllable illumination. All images are captured in linear color space (HDR for synthetic data, camera RAW for real captures) to ensure the photometric linearity required for accurate light composition. We then generate arbitrary lighting conditions by linearly combining these captures with per-light color and intensity coefficients sampled in Lab space. We impose the constraint that the lights being modified must be visible in at least one view, set as the *reference* view, while the second view may or may not have direct visibility of the modified light sources. For our control, we generate a lightmap for the reference view: a mask with colored circles placed at the spatial location of each modified light source, encoding the target color and intensity.

Our dataset comprises three sources with complementary objectives: (i) 365 *Infinigen* [51] scenes to help the model leverage pretrained scene geometry priors; (ii) 40 *BlenderKit*[‡] scenes to provide higher realism, furniture, and light sources; and (iii) *Real* captures from 40 scenes to bridge the domain gap between synthetic and real-world data. In total, the SyncLight Dataset contains nearly one million multi-view training pairs: 920,000 from Infinigen, 47,000 from BlenderKit, and 18,000 from real captures. For testing, we hold out a diverse subset of scenes not seen during training. Detailed capture protocols, light composition equations, and exemplar images for each split are provided in the Supplementary. We will release the full dataset to the community.

5 Experiments

Results and comparisons. LuxRemix [38] and GR3EN [58] (concurrent works) address multi-view relighting, but their code and models are not available. No other prior works offer this capability directly, so we evaluate baseline methods using various adaptations of state-of-the-art methods.

For single-view relighting of the reference view, we compare against (i) ScribbleLight [10] using Marigold [27, 28] to obtain the albedo and depth, and (ii) our own implementation of LightLab [45] (**LightLab***). Given that the original model and data are not publicly available, we closely follow the reported design, including a fine-tuned SDXL backbone conditioned on parametric light masks and the original single-view training objective. To ensure a fair comparison, we train our reproduction on the same dataset used for SyncLight, excluding the multi-view component, allowing us to isolate the effect of multi-view modeling. LightLab* serves as our primary single-view baseline and, to the best of our knowledge, represents the current state-of-the-art for parametric single-view relighting. For relighting the second view, we adopt LumiNet [57] (LNet), using the second view as input and the relit version of the reference view as the reference.

[‡]https://www.blenderkit.com/

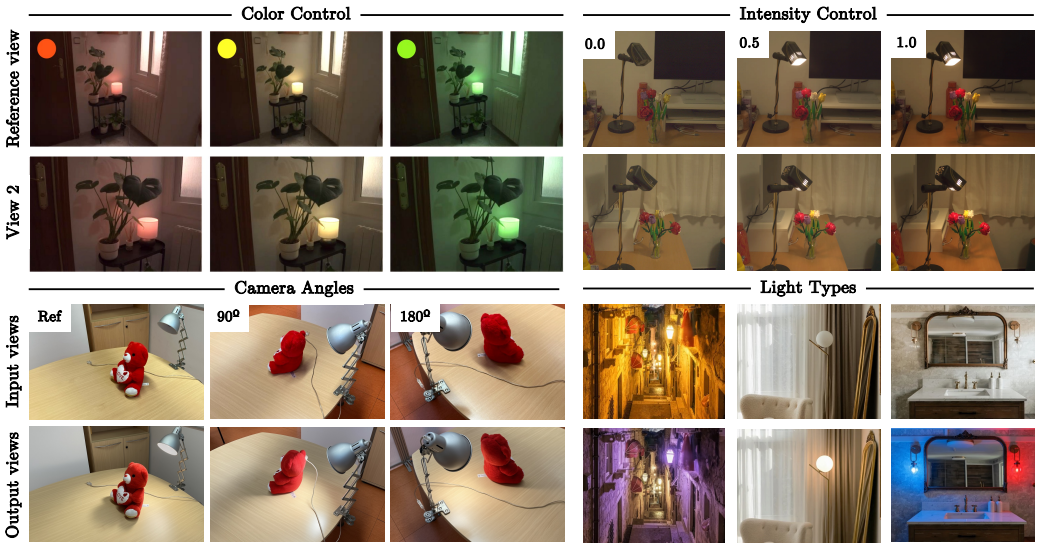


Figure 3: Qualitative results showcasing SyncLight's controllability and generalization. **Top-left:** precise control over light color, varying the chromaticity of a table lamp across three target hues. **Top-right:** continuous control over light intensity, from off (0.0) to fully on (1.0). **Bottom-left:** robustness to large camera angle changes, with input views rotated by up to 180° relative to the reference. **Bottom-right:** generalization across diverse scenes and unseen light types. SyncLight produces consistent relighting across all viewpoints.

We additionally compare against Flux.2-dev [32], a large-scale text-conditioned image editing model. Since it lacks native multi-view support, we implement a two-stage pipeline: we use Qwen-2.5-7B-Instruct [4] to generate a text prompt describing the desired lighting change from the source and target reference views, apply Flux.2-dev to relight the reference view, and then relight the second view by conditioning Flux.2-dev on the relit reference.

As shown in tab. 1 ("Reference (Ref.) view" and "Second (Sec.) view"), our method outperforms previous approaches by a large margin both on the reference and second views. Several key observations emerge from these results. First, SyncLight improves upon Lightlab* on the reference view, indicating that incorporating a second view enhances performance even for single-view relighting. Second, the results for both views in SyncLight are extremely close, clearly indicating the method's ability to consistently match the illumination conditions imposed for the first view with those in the second view. Finally, the average inference time across all images in our dataset demonstrates that our method achieves the most efficient relighting for both views.

SyncLight enables parametric control over light intensity and chromaticity, and generalizes to diverse scenes and light sources. Fig. 3 illustrates four scenarios. **Color Control** (top-left): SyncLight varies the chromaticity of a table lamp across three target hues at fixed intensity, with color bleed on the wall, plant, and floor propagating consistently to View 2. **Intensity Control** (top-right): smooth brightness modulation of a desk lamp from 0.0 to 1.0, with shadows cast by the flowers and vase sharpening coherently across both views. **Camera Angles** (bottom-left): given views rotated by approximately 90° and 180° around the scene, SyncLight produces coherent outputs in which the shadow direction rotates with the camera, suggesting that the model reasons about shadow geometry rather than copying lighting cues from nearby viewpoints. **Light Types** (bottom-right): generalization to diverse, unseen light sources while preserving the rest of the scene.

Qualitative results. Fig. 4 shows qualitative results of competing methods and our SyncLight for the Real split of our dataset. As our dataset is color calibrated, we also present the GT on the last column. Results demonstrate our method's key capabilities: (1) Precise light manipulation: SyncLight correctly modifies individual light sources while preserving the remaining illumination, (2) Multi-view consistency: lighting edits propagate coherently across viewpoints, and (3) Indirect effects: SyncLight plausibly synthesizes indirect illumination effects such as wall reflections and color bleeding. In contrast, Flux.2-dev struggles with cross-view consistency, producing visually plausible but geometrically inconsistent results. The LightLab*+LumiNet baseline, while maintaining better consistency by explicitly relighting each view, fails to propagate lighting effects.



Figure 4: Results in the Real Split from our dataset. SyncLight relights the images correctly. Flux.2-dev struggles with cross-view consistency, producing visually plausible but geometrically inconsistent results (e.g., the window in the second row). Meanwhile, the LightLab*+LumiNet baseline maintains better consistency by explicitly relighting each view, but fails to propagate lighting effects.

Figure 5: Distribution of inter-view angles between reference and second view across our test split (red bars), overlaid with average PSNR per bin (blue curve).

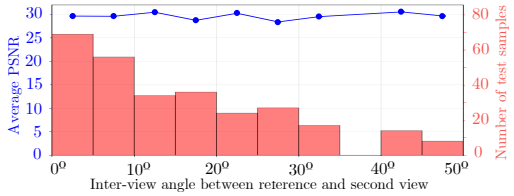


Table 2: Ablation studies. Average results on the "Second view" of the *Real* split of our dataset.

	PSNR	SSIM	ΔE_{00}	LPIPS
w/o *Infinigen*	26.91	.863	4.59	.281
w/o *BlenderKit*	27.29	.872	4.42	.247
w/o *Real*	25.61	.860	4.92	.238
w/o MV-SD	22.47	.833	5.03	.236
SyncLight	30.23	.897	3.56	.197

Inter-view angle performance analysis. A natural concern with multi-view relighting is whether performance degrades as the inter-view angle between the reference and the second view grows. To evaluate this, we bin the pairs of all test scenes by the angular displacement between the reference and second view, and report the average PSNR within each bin. Fig. 5 shows the resulting distribution (in red) and the average PSNR within each bin (blue curve). Importantly, the average PSNR remains essentially flat across the entire range, indicating that SyncLight maintains consistent relighting quality even for wide-baseline pairs.

Ablation studies. Tab. 2 presents ablation experiments. Dataset splits: Removing any split degrades performance on the real test split, with *Infinigen* (-3.3 dB in PSNR), *BlenderKit* (-2.9 dB in PSNR), and *Real* (-4.6 dB in PSNR). Multi-view transformer: Replacing multi-view blocks with standard single-view processing causes severe degradation on "Second view" (-7.7 dB in PSNR), reducing performance significantly. Without cross-view attention, the model cannot propagate lighting to other views, confirming that feature exchange across views is critical for multi-view consistency.

User study. We conducted a 20-participant user study evaluating relighting accuracy, multi-view consistency, and overall quality. Participants compared SyncLight, Flux.2-dev, and LightLab*, the latter provided with an additional lightmap for the second view. SyncLight was preferred in 73.9%, 81.1%, and 81.7% of cases, respectively, indicating superior perceptual quality and cross-view coherence. See supplementary material for details.

Zero-shot multi-view generalization. A crucial property of SyncLight is its ability to generalize zero-shot to an arbitrary number of views, despite being trained exclusively on image pairs ($N = 2$). This capability stems from our multi-view transformer architecture: because cross-view attention operates at the token level rather than being constrained to a fixed number of views, the learned consistency priors naturally extend to larger camera arrays. Fig. 6 presents an example with $N = 7$ views, demonstrating consistent relighting across all views despite exceeding the training configuration. Notably, the modified light source is occluded in views 2 and 4, yet the model correctly



Figure 6: Relighting a scene with seven different views. Top row: Input images. Bottom row: SyncLight results. Note how all the views are consistently modified. We want to emphasize views 2 and 4, in which the lamp turned on is not visible, yet the effects in the scene match those of the other views.



Figure 7: Qualitative results on out-of-distribution images from the RealEstate10K dataset [18]. SyncLight outperforms all the other methods, including a per-view informed version of LightLab*, demonstrating that the joint processing of all views is beneficiary even for single-light relighting.

propagates the lighting changes based on geometric cues from other views. Morover, at 2K resolution, each additional view requires only 0.01GB VRAM and 1.23 seconds on an NVIDIA A40.

We quantitatively evaluate this generalization capability in tab. 1 (*Add. views*). For each image pair in our test set, we randomly sample additional views, obtaining an average of 4.38 views per scene. Baseline methods require a separate forward pass for each additional view, always using the first view as a reference. In contrast, SyncLight processes all views in a single forward pass. Our method maintains consistent relighting quality across the reference view, second view, and all additional views, demonstrating robust multi-view consistency beyond the training distribution.

Out-of-distribution scenes. We additionally evaluate on RealEstate10K [18] on fig. 7, a large-scale collection of indoor video sequences captured with moving cameras across diverse real estate scenes. Although RealEstate10K provides multiple views of the same scene, it lacks ground-truth relighting annotations, and we therefore use it for qualitative evaluation only. Fig. 7 shows that SyncLight generalizes to these unseen, in-the-wild scenes, producing consistent relighting across viewpoints despite the domain shift from our training data. In the scene the camera displacement is huge, and SyncLight is able to turn on the table lamp correctly. SyncLight is the only method that is able to perform the edits correctly. Note that our method also outperforms a per-view variant of LightLab*, where we relit each view independently, providing an additional lightmap for the second view.

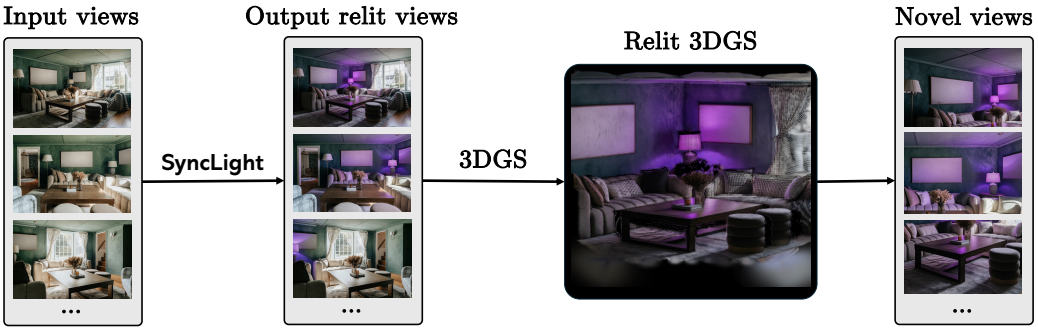
6 Applications

SyncLight is trained on pairs of views $N = 2$. However, in the main manuscript, we show how our approach generalizes zero-shot to multiple views $N > 2$. We always aim at sparse view scenarios where the synchronous views are have a displacement between them. Having said this, there are two applications in which SyncLight is useful: video relighting and 3D relighting. See the attached video to visualize the results for both applications.

Video relighting SyncLight can efficiently relight videos while maintaining temporal consistency, even if it is trained only on *image pairs*. Note that the user only needs to specify the desired lighting condition on the first frame of the video, and SyncLight propagates the light changes across all the following frames. Fig. 8a shows five frames from a 142-frame video from the RealEstate10k dataset [18] alongside their relit versions, demonstrating consistent relighting across all frames. Notably, all 142 frames are processed jointly in a single forward pass, requiring only 156 seconds and 27 GB of VRAM.



(a) Video relighting. From user inputs in the first frame only, SyncLight automatically relights 142 frames of a video from the RealEstate10k dataset [18].



(b) Novel-view synthesis. 3DGS [29] is applied to images relit by SyncLight, which achieves out-of-the-box multi-view consistency.

Figure 8: SyncLight applied to: (a) very wide baseline images, (b) video relighting, and (c) novel-view synthesis with radiance fields. Please see the supplementary video on our webpage.

Novel view synthesis with radiance fields Relighting in radiance field representations (NeRFs, or 3DGS) is inherently challenging since it typically involves complex inverse rendering (e.g., [24]). SyncLight's view-consistent relighting enables an alternative approach: users can relight multiple 2D views and reconstruct the 3D scene, effectively using our method as a proxy for 3D relighting. Fig. 8b and the supplementary video show an example using 3DGS [29] implementation from NerfStudio [56]. Note that, as opposed to Poirier-Ginter et al. [50], no multi-view consistency optimization was performed: we simply used vanilla 3DGS directly on the images relit by SyncLight.

7 Discussion

We presented SyncLight, a method for consistently controlling light sources across multiple uncalibrated views from a single reference edit, achieving strong qualitative and quantitative performance. However, our work has limitations that suggest avenues for future research. First, SyncLight relies on a circular region for light conditioning and may struggle with rare or unconventional light sources; in particular, our work does not target windows. Finer-grained segmentation masks, as in LightLab [45], could improve generalization to such cases at the cost of increased interaction complexity. Second, leveraging priors from video models [37] could enable better generalization to videos, although such approaches may not transfer well to sparse multi-view sets with large baselines, such as those in RealEstate10K. Finally, incorporating 3D priors such as depth or camera pose may further improve performance and broaden generalization. We leave these directions to future work; despite these limitations, SyncLight operates effectively on wide-baseline stereo setups and demonstrates zero-shot generalization across multiple cameras without relying on 3D information. We are confident that SyncLight marks the beginning of a broader research direction in multi-view, synchronous relighting.

Broader impact statement Improved relighting models benefit content creation, AR, and VFX by enabling realistic lighting edits. The proposed method is a fundamental research contribution and does not have a direct negative societal impact; however, as with all image generation technologies, downstream applications must prioritize ethical use and guard against potential misuse.

References

[1] Yagiz Aksoy, Changil Kim, Petr Kellnhofer, Sylvain Paris, Mohamed Elgharib, Marc Pollefeys, and Wojciech Matusik. A dataset of flash and ambient illumination pairs from the crowd. In *Eur. Conf. Comput. Vis.*, 2018.

[2] Michael Albergo, Nicholas M Boffi, and Eric Vanden-Eijnden. Stochastic interpolants: A unifying framework for flows and diffusions. *J. Mach. Learn. Research*, 26(209):1–80, 2025.

[3] Hadi Alzayer, Philipp Henzler, Jonathan T. Barron, Jia-Bin Huang, Pratul P. Srinivasan, and Dor Verbin. Generative multiview relighting for 3d reconstruction under extreme illumination variation. In *IEEE/CVF Conf. Comput. Vis. Pattern Recog.*, 2025.

[4] Jinze Bai, Shuai Bai, Yunfei Chu, Zeyu Cui, Kai Dang, Xiaodong Deng, Yang Fan, Wenbin Ge, Yu Han, Fei Huang, et al. Qwen technical report. *arXiv preprint arXiv:2309.16609*, 2023.

[5] Shrisha Bharadwaj, Haiwen Feng, Giorgio Becherini, Victoria Fernandez Abrevaya, and Michael J Black. Genlit: Reformulating single-image relighting as video generation. In *ACM SIGGRAPH Asia Conf.*, 2025.

[6] Anand Bhattad, Daniel McKee, Derek Hoiem, and David Forsyth. StyleGAN knows normal, depth, albedo, and more. In *Adv. Neural Inform. Process. Syst.*, 2023.

[7] Anand Bhattad, James Soole, and David A. Forsyth. Stylitgan: Image-based relighting via latent control. In *IEEE/CVF Conf. Comput. Vis. Pattern Recog.*, 2024.

[8] Chris Careaga and Yağız Aksoy. Physically controllable relighting of photographs. In *ACM SIGGRAPH Conf.*, 2025.

[9] Clément Chadebec, Onur Tasar, Sanjeev Sreetharan, and Benjamin Aubin. Lbm: Latent bridge matching for fast image-to-image translation. In *IEEE/CVF Int. Conf. Comput. Vis.*, 2025.

[10] Jun Myeong Choi, Annie Wang, Pieter Peers, Anand Bhattad, and Roni Sengupta. Scribblelight: Single image indoor relighting with scribbles. In *IEEE/CVF Conf. Comput. Vis. Pattern Recog.*, 2025.

[11] Kangle Deng, Timothy Omernick, Alexander Weiss, Deva Ramanan, Jun-Yan Zhu, Tinghui Zhou, and Maneesh Agrawala. Flashtex: Fast relightable mesh texturing with lightcontrolnet. In *Eur. Conf. Comput. Vis.*, 2024.

[12] Xiaodan Du, Nicholas Kolkin, Greg Shakhnarovich, and Anand Bhattad. Generative models: What do they know? do they know things? let's find out! *arXiv preprint arXiv:2311.17137*, 2023.

[13] Yotam Erel, Rishabh Dabral, Vladislav Golyanik, Amit H. Bermano, and Christian Theobalt. Practilight: Practical light control using foundational diffusion models. *ACM Transactions on Graphics (TOG)*, 44(6):1–11, 2025.

[14] Ye Fang, Zeyi Sun, Shangzhan Zhang, Tong Wu, Yinghao Xu, Pan Zhang, Jiaqi Wang, Gordon Wetzstein, and Dahua Lin. Relightvid: Temporal-consistent diffusion model for video relighting. *arXiv preprint arXiv:2501.16330*, 2025.

[15] Frédéric Fortier-Chouinard, Zitian Zhang, Louis-Etienne Messier, Mathieu Garon, Anand Bhattad, and Jean-François Lalonde. Spotlight: Shadow-guided object relighting via diffusion. In *Int. Conf. 3D Vis.*, 2026.

[16] James Gardner, Evgenii Kashin, Bernhard Egger, and William Alfred Peter Smith. The sky's the limit: Relightable outdoor scenes via a sky-pixel constrained illumination prior and outside-in visibility. In *Eur. Conf. Comput. Vis.*, 2024.

[17] Marc-André Gardner, Yannick Hold-Geoffroy, Kalyan Sunkavalli, Christian Gagné, and Jean-François Lalonde. Deep parametric indoor lighting estimation. In *IEEE/CVF Int. Conf. Comput. Vis.*, 2019.

[18] Google Research. RealEstate10K: A large-scale dataset of camera poses. `https://google.github.io/realestate10k/`, 2018.

[19] Kai He, Ruofan Liang, Jacob Munkberg, Jon Hasselgren, Nandita Vijaykumar, Alexander Keller, Sanja Fidler, Igor Gilitschenski, Zan Gojcic, and Zian Wang. Unirelight: Learning joint decomposition and synthesis for video relighting. In *Adv. Neural Inform. Process. Syst.*, 2025.

[20] Mingming He, Pascal Clausen, Ahmet Levent Taşel, Li Ma, Oliver Pilarski, Wenqi Xian, Laszlo Rikker, Xueming Yu, Ryan Burgert, Ning Yu, et al. Diffrelight: Diffusion-based facial performance relighting. In *ACM SIGGRAPH Asia Conf.*, 2024.

[21] Paul Heckbert. Synthetic lighting for photography, 1996. Accessed: 2025-09-17.

[22] Zhuo Hui, Kalyan Sunkavalli, Sunil Hadap, and Aswin C Sankaranarayanan. Illuminant spectra-based source separation using flash photography. In *IEEE/CVF Conf. Comput. Vis. Pattern Recog.*, 2018.

[23] Haian Jin, Yuan Li, Fujun Luan, Yuanbo Xiangli, Sai Bi, Kai Zhang, Zexiang Xu, Jin Sun, and Noah Snavely. Neural gaffer: Relighting any object via diffusion. In *Adv. Neural Inform. Process. Syst.*, 2024.

[24] Haian Jin, Isabella Liu, Peijia Xu, Xiaoshuai Zhang, Songfang Han, Sai Bi, Xiaowei Zhou, Zexiang Xu, and Hao Su. Tensoir: Tensorial inverse rendering. In *IEEE/CVF Conf. Comput. Vis. Pattern Recog.*, 2023.

[25] Kevin Karsch, Varsha Hedau, David Forsyth, and Derek Hoiem. Rendering synthetic objects into legacy photographs. *ACM Trans. Graph.*, 2011.

[26] Kevin Karsch, Kalyan Sunkavalli, Sunil Hadap, Nathan Carr, Hailin Jin, Rafael Fonte, Michael Sittig, and David Forsyth. Automatic scene inference for 3d object compositing. *ACM Trans. Graph.*, 2014.

[27] Bingxin Ke, Anton Obukhov, Shengyu Huang, Nando Metzger, Rodrigo Caye Daudt, and Konrad Schindler. Repurposing diffusion-based image generators for monocular depth estimation. In *IEEE/CVF Conf. Comput. Vis. Pattern Recog.*, 2024.

[28] Bingxin Ke, Kevin Qu, Tianfu Wang, Nando Metzger, Shengyu Huang, Bo Li, Anton Obukhov, and Konrad Schindler. Marigold: Affordable adaptation of diffusion-based image generators for image analysis. *IEEE Trans. Pattern Anal. Mach. Intell.*, pages 1–18, 2025.

[29] Bernhard Kerbl, Georgios Kopanas, Thomas Leimkühler, and George Drettakis. 3d gaussian splatting for real-time radiance field rendering. *ACM Trans. Graph.*, 42(4):139–1, 2023.

[30] Peter Kocsis, Julien Philip, Kalyan Sunkavalli, Matthias Nießner, and Yannick Hold-Geoffroy. Lightit: Illumination modeling and control for diffusion models. In *IEEE/CVF Conf. Comput. Vis. Pattern Recog.*, 2024.

[31] Peter Kocsis, Vincent Sitzmann, and Matthias Nießner. Intrinsic image diffusion for single-view material estimation. In *IEEE/CVF Conf. Comput. Vis. Pattern Recog.*, 2024.

[32] Black Forest Labs. FLUX.2: Frontier Visual Intelligence. `https://bfl.ai/blog/flux-2`, 2025.

[33] Junxuan Li, Hongdong Li, and Yasuyuki Matsushita. Lighting, reflectance and geometry estimation from 360° panoramic stereo. In *IEEE/CVF Conf. Comput. Vis. Pattern Recog.*, 2021.

[34] Zhen Li, Lingli Wang, Mofang Cheng, Cihui Pan, and Jiaqi Yang. Multi-view inverse rendering for large-scale real-world indoor scenes. In *IEEE/CVF Conf. Comput. Vis. Pattern Recog.*, 2023.

[35] Zhengqin Li, Mohammad Shafiei, Ravi Ramamoorthi, Kalyan Sunkavalli, and Manmohan Chandraker. Inverse rendering for complex indoor scenes: Shape, spatially-varying lighting and svbrdf from a single image. In *IEEE/CVF Conf. Comput. Vis. Pattern Recog.*, 2020.

[36] Zhengqin Li, Jia Shi, Sai Bi, Rui Zhu, Kalyan Sunkavalli, Miloš Hašan, Zexiang Xu, Ravi Ramamoorthi, and Manmohan Chandraker. Physically-based editing of indoor scene lighting from a single image. In *Eur. Conf. Comput. Vis.*, 2022.

[37] Ruofan Liang, Zan Gojcic, Huan Ling, Jacob Munkberg, Jon Hasselgren, Zhi-Hao Lin, Jun Gao, Alexander Keller, Nandita Vijaykumar, Sanja Fidler, and Zian Wang. Diffusionrenderer: Neural inverse and forward rendering with video diffusion models. In *IEEE/CVF Conf. Comput. Vis. Pattern Recog.*, June 2025.

[38] Ruofan Liang, Norman Müller, Ethan Weber, Duncan Zauss, Nandita Vijaykumar, Peter Kontschieder, and Christian Richardt. Luxremix: Lighting decomposition and remixing for indoor scenes. In *IEEE/CVF Conf. Comput. Vis. Pattern Recog.*, 2026.

[39] Zhi-Hao Lin, Bohan Liu, Yi-Ting Chen, Kuan-Sheng Chen, David Forsyth, Jia-Bin Huang, Anand Bhattad, and Shenlong Wang. Urbanir: Large-scale urban scene inverse rendering from a single video. In *Int. Conf. 3D Vis.*, 2025.

[40] Yaron Lipman, Ricky T. Q. Chen, Heli Ben-Hamu, Maximilian Nickel, and Matthew Le. Flow matching for generative modeling. In *Int. Conf. Learn. Represent.*, 2023.

[41] Yehonathan Litman, Fernando De la Torre, and Shubham Tulsiani. Lightswitch: Multi-view relighting with material-guided diffusion. In *IEEE/CVF Int. Conf. Comput. Vis.*, 2025.

[42] Xingchao Liu, Chengyue Gong, and Qiang Liu. Flow straight and fast: Learning to generate and transfer data with rectified flow. In *Int. Conf. Learn. Represent.*, 2023.

[43] Xiaoxiao Long, Yuan-Chen Guo, Cheng Lin, Yuan Liu, Zhiyang Dou, Lingjie Liu, Yuexin Ma, Song-Hai Zhang, Marc Habermann, Christian Theobalt, et al. Wonder3d: Single image to 3d using cross-domain diffusion. In *IEEE/CVF Conf. Comput. Vis. Pattern Recog.*, 2024.

[44] Linjie Lyu, Valentin Deschaintre, Yannick Hold-Geoffroy, Miloš Hašan, Jae Shin Yoon, Thomas Leimküehler, Christian Theobalt, and Iliyan Georgiev. Intrinsicedit: Precise generative image manipulation in intrinsic space. *ACM Trans. Graph.*, 44(4), 2025.

[45] Nadav Magar, Amir Hertz, Eric Tabellion, Yael Pritch, Alex Rav-Acha, Ariel Shamir, and Yedid Hoshen. Lightlab: Controlling light sources in images with diffusion models. In *ACM SIGGRAPH Conf.*, 2025.

[46] Yiqun Mei, Mingming He, Li Ma, Julien Philip, Wenqi Xian, David M George, Xueming Yu, Gabriel Dedic, Ahmet Levent Taşel, Ning Yu, et al. Lux post facto: Learning portrait performance relighting with conditional video diffusion and a hybrid dataset. In *IEEE/CVF Conf. Comput. Vis. Pattern Recog.*, 2025.

[47] Ben Mildenhall, Pratul P Srinivasan, Matthew Tancik, Jonathan T Barron, Ravi Ramamoorthi, and Ren Ng. NeRF: Representing scenes as neural radiance fields for view synthesis. *Communications of the ACM*, 65(1):99–106, 2021.

[48] Lukas Murmann, Michael Gharbi, Miika Aittala, and Fredo Durand. A dataset of multi-illumination images in the wild. In *IEEE/CVF Int. Conf. Comput. Vis.*, 2019.

[49] Dustin Podell, Zion English, Kyle Lacey, Andreas Blattmann, Tim Dockhorn, Jonas Müller, Joe Penna, and Robin Rombach. SDXL: Improving latent diffusion models for high-resolution image synthesis. In *Int. Conf. Learn. Represent.*, 2024.

[50] Yohan Poirier-Ginter, Alban Gauthier, Julien Phillip, J-F Lalonde, and George Drettakis. A diffusion approach to radiance field relighting using multi-illumination synthesis. *Comput. Graph. Forum*, 43(4), 2024.

[51] Alexander Raistrick, Lingjie Mei, Karhan Kayan, David Yan, Yiming Zuo, Beining Han, Hongyu Wen, Meenal Parakh, Stamatis Alexandropoulos, Lahav Lipson, et al. Infinigen indoors: Photorealistic indoor scenes using procedural generation. In *IEEE/CVF Conf. Comput. Vis. Pattern Recog.*, 2024.

[52] Robin Rombach, Andreas Blattmann, Dominik Lorenz, Patrick Esser, and Björn Ommer. High-resolution image synthesis with latent diffusion models. In *IEEE/CVF Conf. Comput. Vis. Pattern Recog.*, 2022.

[53] Yichun Shi, Peng Wang, Jianglong Ye, Long Mai, Kejie Li, and Xiao Yang. MVDream: Multi-view diffusion for 3d generation. In *Int. Conf. Learn. Represent.*, 2024.

[54] Yuyang Shi, Valentin De Bortoli, Andrew Campbell, and Arnaud Doucet. Diffusion Schrödinger bridge matching. In *Adv. Neural Inform. Process. Syst.*, 2023.

[55] Zhenxiong Tan, Zeqing Wang, Xingyi Yang, Songhua Liu, and Xinchao Wang. Vision bridge transformer at scale. *arXiv preprint arXiv:2511.23199*, 2025.

[56] Matthew Tancik, Ethan Weber, Evonne Ng, Ruilong Li, Brent Yi, Terrance Wang, Alexander Kristoffersen, Jake Austin, Kamyar Salahi, Abhik Ahuja, et al. Nerfstudio: A modular framework for neural radiance field development. In *ACM SIGGRAPH Conf.*, 2023.

[57] Xiaoyan Xing, Konrad Groh, Sezer Karagolu, Theo Gevers, and Anand Bhattad. Luminet: Latent intrinsics meets diffusion models for indoor scene relighting. In *IEEE/CVF Conf. Comput. Vis. Pattern Recog.*, 2025.

[58] Xiaoyan Xing, Philipp Henzler, Junhwa Hur, Runze Li, Jonathan T Barron, Pratul P Srinivasan, and Dor Verbin. Gr3en: Generative relighting for 3d environments. In *ACM SIGGRAPH Conf.*, 2026.

[59] Zongsheng Yue, Jianyi Wang, and Chen Change Loy. Resshift: Efficient diffusion model for image super-resolution by residual shifting. In *Adv. Neural Inform. Process. Syst.*, 2023.

[60] Chong Zeng, Yue Dong, Pieter Peers, Youkang Kong, Hongzhi Wu, and Xin Tong. Dilightnet: Fine-grained lighting control for diffusion-based image generation. In *ACM SIGGRAPH Conf.*, 2024.

[61] Zheng Zeng, Valentin Deschaintre, Iliyan Georgiev, Yannick Hold-Geoffroy, Yiwei Hu, Fujun Luan, Ling-Qi Yan, and Miloš Hašan. RGB↔X: Image decomposition and synthesis using material-and lighting-aware diffusion models. In *ACM SIGGRAPH Conf.*, 2024.

[62] Edward Zhang, Michael F. Cohen, and Brian Curless. Emptying, refurnishing, and relighting indoor spaces. *ACM Trans. Graph.*, 35(6), 2016.

[63] Lvmin Zhang, Anyi Rao, and Maneesh Agrawala. Scaling in-the-wild training for diffusion-based illumination harmonization and editing by imposing consistent light transport. In *Int. Conf. Learn. Represent.*, 2025.

[64] Richard Zhang, Phillip Isola, Alexei A. Efros, Eli Shechtman, and Oliver Wang. The unreasonable effectiveness of deep features as a perceptual metric. In *IEEE/CVF Conf. Comput. Vis. Pattern Recog.*, 2018.

[65] Xiao Zhang, William Gao, Seemandhar Jain, Michael Maire, David Forsyth, and Anand Bhattad. Latent intrinsics emerge from training to relight. In *Adv. Neural Inform. Process. Syst.*, 2024.

[66] Zitian Zhang, Frédéric Fortier-Chouinard, Mathieu Garon, Anand Bhattad, and Jean-François Lalonde. Zerocomp: Zero-shot object compositing from image intrinsics via diffusion. In *IEEE/CVF Winter Conf. App. Comput. Vis.*, 2025.

[67] Xiaoming Zhao, Pratul P. Srinivasan, Dor Verbin, Keunhong Park, Ricardo Martin Brualla, and Philipp Henzler. Illuminerf: 3d relighting without inverse rendering. In *Adv. Neural Inform. Process. Syst.*, 2024.

[68] Jingsen Zhu, Yuchi Huo, Qi Ye, Fujun Luan, Jifan Li, Dianbing Xi, Lisha Wang, Rui Tang, Wei Hua, Hujun Bao, and Rui Wang. I^2-sdf: Intrinsic indoor scene reconstruction and editing via raytracing in neural sdfs. In *IEEE/CVF Conf. Comput. Vis. Pattern Recog.*, 2023.

A Dataset details

Comparison with existing datasets. Existing datasets fall short of the three criteria required for multi-view relighting (diverse indoor geometry, synchronised multi-view captures, and isolated controllable light sources). The Multi-Illumination dataset [48], while offering real-world lighting variations, does not contain consistent multi-view captures or visible light sources, preventing its use for multi-view propagation. The dataset used by LightLab [45] is single-view only and is not publicly available. These limitations motivate the construction of the SyncLight dataset.

Light composition pipeline. We first obtain an ambient image I_{amb} with all controllable lights turned off, capturing only ambient illumination. Then, we render (or capture) the scene lit by each of the N light sources individually following the OLAT protocol, yielding a set of images $\{I_i\}$ for light $i \in \{1, ..., M\}$. By subtracting the ambient light from each OLAT capture, we obtain the isolated contribution of each light source: $L_i = I_i - I_{\text{amb}}$. We can then generate arbitrary lighting combinations with different intensities and colors through weighted linear combinations:

$$I_{\text{relit}} = I_{\text{amb}} + \sum_{i=1}^{M} c_i L_i \,, \tag{5}$$

where $c_i \in \mathbb{R}^3$ specifies the desired color (and intensity) of light i. In practice, c_i is originally defined in Lab space as to more intuitively separate luminance from chromaticity and then converted to RGB before applying the combination. Finally, we apply tone mapping to convert the linear result to a non-linear 8-bit image. We use Reinhard method with a $\gamma = 2.2$.

Dataset sources. Our dataset presents images from three different sources: Infinigen, BlenderKit, and Real captures. Infinigen images enable the model to leverage pretrained scene-geometry priors across views. BlenderKit images contribute increased realism, including furniture and light sources. Finally, Real capture images help reduce the domain gap between synthetic and real-world data.

Infinigen. We utilize Infinigen [51], a procedural generator of photorealistic 3D Blender scenes, to create 365 diverse indoor environments across five room types: bathrooms, bedrooms, living rooms, dining rooms, and kitchens. Each scene exhibits high variation in geometry, materials, and assets. We procedurally place 5 camera groups, each comprising 5 cameras, pointing at different parts of the scene. We ensure at least 25% spatial overlap between all viewpoints within the same group to maintain multi-view consistency constraints. For each scene, we identify all emissive objects (e.g., lamps and ceiling lights) and render them following the OLAT protocol. Each view is rendered in HDR with physically-based rendering, producing a total of 920,000 pairs of different lighting combinations.

BlenderKit. To increase realism beyond procedurally-generated scenes, we curate 40 high-quality Blender scenes from BlenderKit[§], a repository of artist-created 3D assets and scenes. These scenes feature more realistic furniture arrangements, diverse architectural styles, and complex lighting fixtures. To integrate these scenes into our pipeline, we perform several preprocessing steps: (i) we replace all emissive materials with transparent materials and explicit Light objects to enable precise OLAT control; (ii) we manually position 3–6 cameras per scene following the same multi-view overlap constraints as *Infinigen*; (iii) we remove unrealistic or low-quality assets; and (iv) we augment scenes with additional BlenderKit assets including diverse lamps, light fixtures, and decorative objects to enhance scene complexity and realism. Each view is rendered in HDR format, similarly to Infinigen, producing 47,000 pairs with diverse lighting combinations.

Real captures. To bridge the gap between synthetic and real-world imagery, we capture 320 RAW photographs from 40 indoor scenes. We use a DSLR camera (Canon EOS 1300D) and a mobile device (iPhone 13), fixed on a tripod and activated via a remote trigger. For each viewpoint, we fix the camera parameters (ISO, shutter speed, and aperture for the DSLR; ISO and shutter speed for the mobile device) to preserve photometric consistency across OLAT captures. Exposure settings are selected to minimize clipping under active lighting while keeping the ambient capture sufficiently bright to avoid excessive noise. We reposition the tripod to acquire multiple viewpoints per scene and capture each scene following the same multi-view OLAT protocol as in the synthetic splits. We then manually annotate light source locations in the images and apply the same light composition pipeline to generate new lighting conditions. This yields 18,000 real-image pairs with diverse lighting configurations.

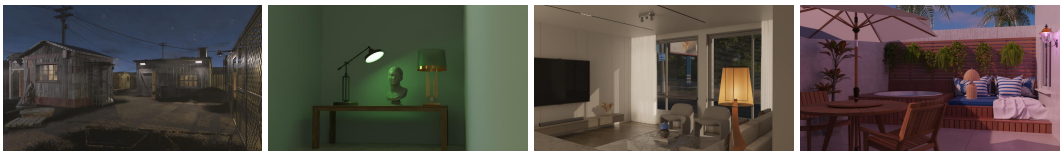
Test split. For testing, we hold out a diverse subset of scenes not seen during training: 10 from Infinigen, 3 from BlenderKit, and 6 from Real captures. From these unseen scenes, we randomly sample a fixed test set of 135, 45, and 105 pairs, respectively. This held-out split is used for all quantitative evaluations reported in the main paper.

Fig. 9 illustrates examples from the SyncLight dataset. Images and light conditions were selected randomly.

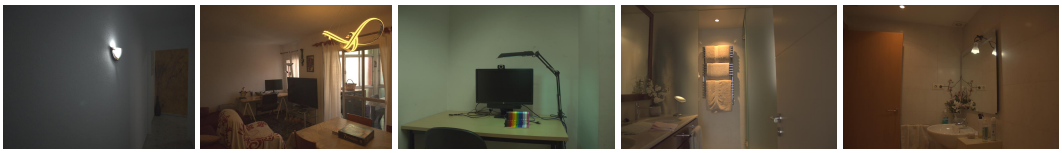
[§]https://www.blenderkit.com/



(a) *Infinigen* split



(b) *BlenderKit* split



(c) *Real* split

Figure 9: Examples from the SyncLight dataset. Samples were selected randomly with random light colors.

B Further method analysis and details

Interpolant stochasticity. Flow matching interpolates between two samples through a deterministic linear combination. In contrast, bridge matching introduces a stochastic component via Gaussian noise:

$$\mathbf{z}_t = (1-t)\mathbf{z}_{src} + t\mathbf{z}_{tar} + \sigma\sqrt{t(1-t)}\boldsymbol{\epsilon}\,, \tag{6}$$

where $\mathbf{z}_{\text{src}}$ and $\mathbf{z}_{\text{tar}}$ are (latent) samples from the source and target distributions, respectively, and $\boldsymbol{\epsilon} \sim \mathcal{N}(0, \mathbf{I})$. The parameter σ controls the level of stochasticity in the interpolant. Tab. 3 evaluates four different values of σ. For each row, we retrain SyncLight using four steps ($T = 4$), but with different values of σ. We find that $\sigma = 0.005$ achieves optimal performance, while both deterministic flow matching ($\sigma = 0$) and higher noise levels ($\sigma > 0.005$) result in degraded performance.

Number of timesteps T during training. We employ four timesteps during training. It is crucial to learn a well-conditioned vector field rather than a brittle point-to-point mapping. As the broader flow matching literature shows [40], training over multiple timesteps yields a generalizable transport, even if inference is truncated to fewer steps [9]. Reducing the number of timesteps to one ($T_{train} = 1$) during training reduces the formulation to an L_2 loss. To validate this, we trained SyncLight using only one timestep during training (using $t = 0$ in eq. (6)). Tab. 4 reports a 4.82dB drop in PSNR on the Real split of our dataset compared to our $T_{train} = 4$ formulation. Multi-step training provides a clear, measurable benefit.

Number of timesteps at inference time. SyncLight is trained with four equally spaced timesteps (t in eq. (6)). Surprisingly, we find that using only a single timestep during inference is both faster and more accurate, as shown in tab. 5. Note that for this experiment, the model weights are the ones obtained using four timesteps during training, and even with that, one-step inference gives better performance. We attribute this counterintuitive result to the initialization strategy. Unlike standard text-to-image models that start from Gaussian noise, our framework begins with the input images as $\mathbf{z}_{\text{src}}$, which already provides a strong initialization. Under this regime, each additional timestep introduces a discretization error that accumulates across the trajectory, ultimately degrading the quality of the final output.

Velocity estimator discussion. We employ Stable Diffusion as the velocity estimator in our bridge matching formulation. While video diffusion models may appear suitable for multi-image processing, their architectures are designed for temporally coherent sequences where consecutive frames exhibit high visual similarity. Our multi-view scenario differs fundamentally: synchronized views from different camera positions contain substantially different visual content despite depicting the same scene. The temporal-encoding mechanisms in video VAEs, optimized for frame-to-frame coherence, struggle to capture this sparse multi-view setting. Instead, we leverage image diffusion models and introduce explicit multi-view reasoning through our transformer-based attention mechanism.

Table 3: Effect of the noise level σ.

	PSNR	SSIM	ΔE_{00}	LPIPS
$\sigma = 0$ (FM)	29.71	.883	3.91	.203
$\sigma = 0.001$	30.03	.884	3.87	.210
$\sigma = 0.005$	30.29	.896	3.65	.196
$\sigma = 0.01$	26.48	.863	4.76	.228

Table 4: Effect of the number of steps during training T. For inference, we use only one timestep on both cases.

	PSNR	SSIM	ΔE_{00}	LPIPS
$T_{train} = 0$	25.47	.858	5.02	.243
$T_{train} = 4$	30.29	.896	3.65	.196

Table 5: Effect of the number of inference steps.

	PSNR	SSIM	ΔE_{00}	LPIPS
One-step	30.29	.896	3.65	.196
Two-step	30.04	.893	3.71	.197
Four-step	29.98	.893	3.74	.200

Table 6: Effect of the color space used for the LBM formulation.

	PSNR	SSIM	ΔE_{00}	LPIPS
RGB	30.09	.894	3.82	.199
CIE Lab	30.29	.896	3.65	.196

Multi-view transformer block further details. SyncLight takes as input two synchronized, uncalibrated views under source lighting, together with a target lighting condition specified on the reference view, and predicts both views under the target lighting. Standard diffusion- and flow-based architectures are designed for single-image inputs and do not model cross-view interactions. We therefore modify the transformer blocks of Stable Diffusion XL to operate in our setting while preserving its pretrained weights. In contrast to text-to-3D methods such as MVDream [53] and Wonder3D [43], our approach does not require camera poses, as we aim at synchronized light source editing rather than 3D generation. The key idea is to enable information exchange across N views through a modified self-attention mechanism (see fig. 10 for an illustration with $N = 2$). Given a batch of N view latents, we first process each view's features independently through the initial convolutional layers. Before each transformer block, features from all views are concatenated along the token dimension rather than the batch dimension, allowing features from different views to interact within the multi-view transformer block. Fig. 11 shows an example with $N = 3$ views, where a table lamp is turned on with a red color and the angle between the reference view and one of the other views reaches up to 90°

Lightmap codification. Finally, we analyze the choice of color space for lightmap encoding. We employ the CIE Lab color space to encode target light colors, as it provides a perceptually uniform color representation. Tab. 6 compares Lab encoding against RGB. While performance is similar, Lab achieves marginally better results and offers user-friendliness. Its inherent separation of luminance (L) and chromaticity (ab) enables independent control over light intensity and color, which is more intuitive for users.

The effect of diverse domains Fig. 12 complements the Ablation study from the main paper, showing qualitative results from our model when each of the dataset splits is removed at a time. In detail, we can see how lamps can lose realism when either the *Real captures* or the *BlenderKit* splits are not used—see the dark color of the ceiling lamp in the bottom figure. In contrast, not using the large number of images from the *Infinigen* split forces the model to output slightly brighter results.

Implementation details. We fine-tune our modified SDXL model [49] for 100,000 steps using a learning rate of 1×10^{-5} and a batch size of 6 at a resolution of 1280×720. Training is performed on six NVIDIA A40 GPUs. $\lambda = 10$ in all experiments.

C User study

Standard image-quality metrics such as PSNR, SSIM, ΔE_{00}, and LPIPS measure pixel- or feature-level distance to a reference image, but do not capture key perceptual aspects of relighting: fidelity to the requested light colour and intensity, plausibility of shadows and inter-reflections, and coherence across viewpoints. We therefore complement our quantitative evaluation with a user study assessing these perceptual qualities directly.

We present the instructions given to participants in fig. 13. Participants were first introduced to the overall layout of the experimental interface through both written instructions and a visual example, and were then given explanations of the three types of questions they would be asked. For each sample, participants were shown a reference view together with a target lighting specification and the corresponding outputs from three methods: SyncLight, LightLab* (provided with a per-view lightmap) [45], and Flux2 [32]. Although our method internally uses CIE Lab, we present the target lighting to participants as an RGB swatch encoding the desired color and intensity, for simplicity. The light source to be manipulated is indicated by a circle marker overlaid

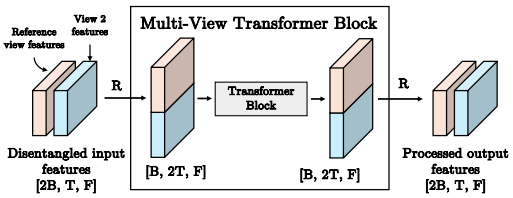


Figure 10: Multi-view transformer block. To ensure consistent relighting across viewpoints, we modify the standard self-attention mechanism of SDXL. View features are concatenated and reshaped along the sequence dimension, creating a unified representation of shape $[B, 2T, F]$



Figure 11: Example of SyncLight with $N = 3$ views. Despite up to $\sim 90^\circ$ between the reference view and the farthest view, SyncLight produces consistent relighting across all viewpoints when turning on a red table lamp.



Figure 12: Multi-view relighting examples when training SyncLight without one of the splits of the dataset at a time.

on the reference view. The order of the three methods was randomized per sample to eliminate position bias. Participants were asked to answer three questions, each targeting a distinct perceptual axis of relighting quality:

1. **Relighting accuracy:** Which output is closest to the target light color and intensity? This question evaluates fidelity to the user-specified edit, independent of considerations of consistency or realism.
2. **Multi-view consistency:** Which output exhibits the most consistent lighting between the two views (e.g., coherent shadow direction, matching color casts, agreement on light source state)? This question isolates the cross-view coherence that distinguishes SyncLight from per-view baselines.
3. **Overall quality:** Which output is the most visually convincing overall? This question captures the holistic perceptual judgement that integrates accuracy, consistency, and the absence of artefacts.

We collected responses from 20 participants, each answering all three questions for 10 samples, yielding 200 votes per question. Fig. 14 summarizes the results. SyncLight is preferred across all three criteria by 73.9% (relighting accuracy), 81.1% (multi-view consistency), and 81.7% (overall quality), with non-overlapping 95% Wilson confidence intervals between SyncLight and the next-best method in every case. Notably, and in line with our motivation and the results in tab. 1, SyncLight outperforms LightLab* in all three criteria despite the latter being provided with a per-view lightmap as additional input. This indicates that jointly processing all views improves not only multi-view consistency but also single-view relighting accuracy, since the model can leverage cross-view evidence (e.g., shading cues visible in one view but not in another) to better estimate the target lighting in each frame. Flux2 achieves results comparable to LightLab* on relighting accuracy, which

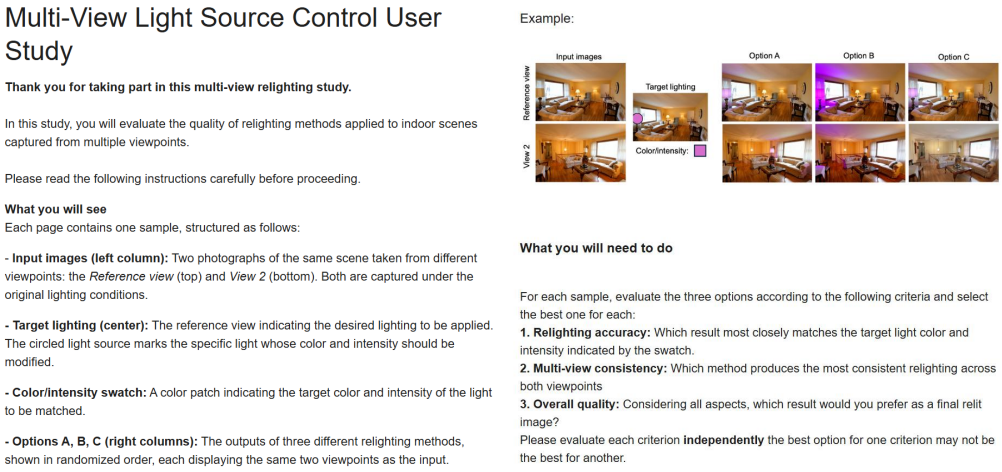


Figure 13: Instructions given to the users for the User Study.

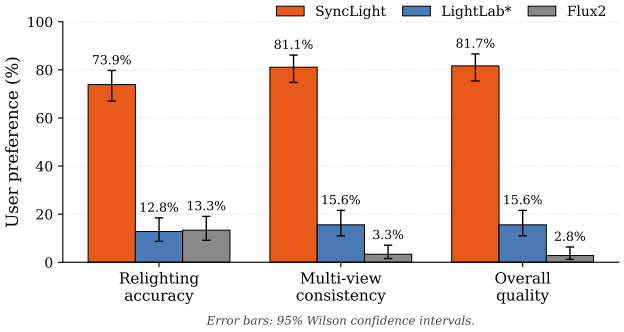


Figure 14: User study results.

we attribute to its strength as a general-purpose image editor capable of producing plausible global colour and contrast adjustments. However, as the consistency and overall quality results show, this comes at the cost of geometric coherence across views and frequently introduces hallucinations or physically implausible artifacts.

D Additional visual results

Fig. 15 shows further qualitative results of competing methods and SyncLight across the Infinigen and BlenderKit splits of our dataset (Real split shown in the main paper), demonstrating the strong performance of our method. In contrast, Flux.2-dev struggles with cross-view consistency, producing visually plausible but geometrically inconsistent results — note the differing lamp colors across views in BlenderKit row 2. The LightLab*+LumiNet baseline, while maintaining better consistency by explicitly relighting each view, fails to propagate lighting effects when sources are not directly visible (BlenderKit row 2, second view).

Fig. 16–fig. 17 present additional results from our method on the RealEstate10K dataset, illustrating various scenarios in which different lights are switched on or off under different colors and intensity conditions.

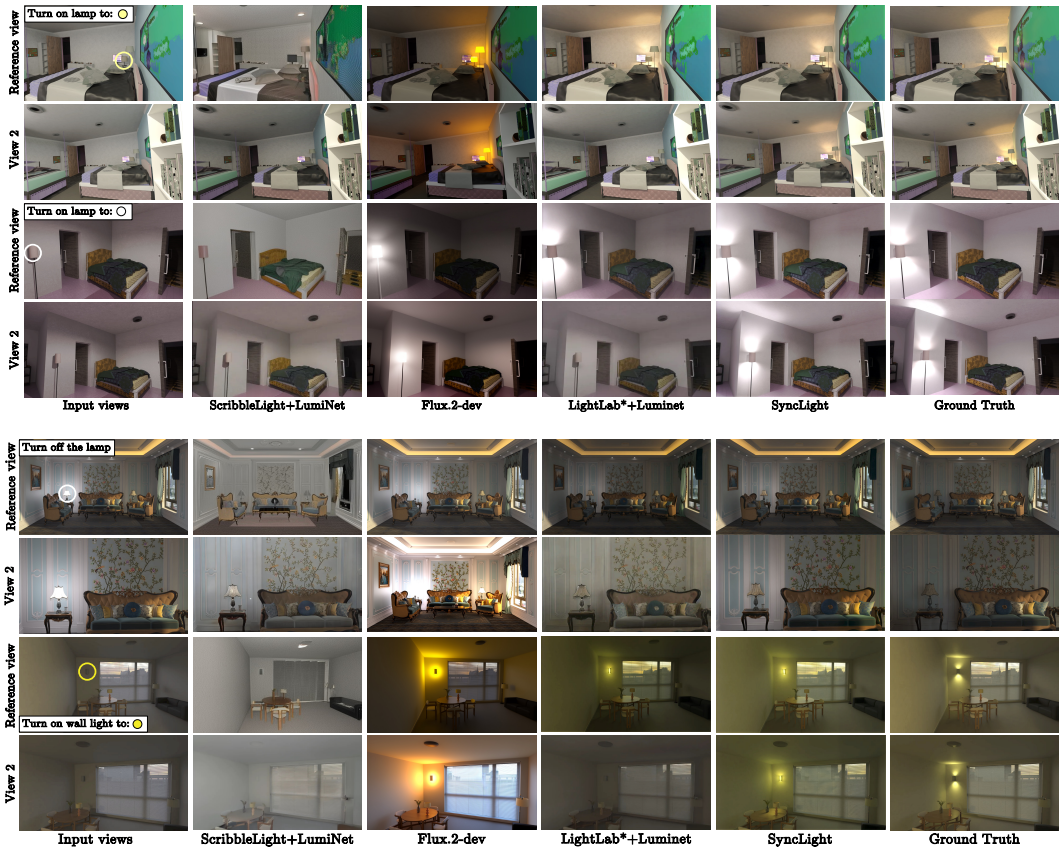


Figure 15: Qualitative results on the SyncLight dataset on the *Infinigen* (1–2), and *BlenderKit* (3–4) splits. *Real* split is shown in the main paper.

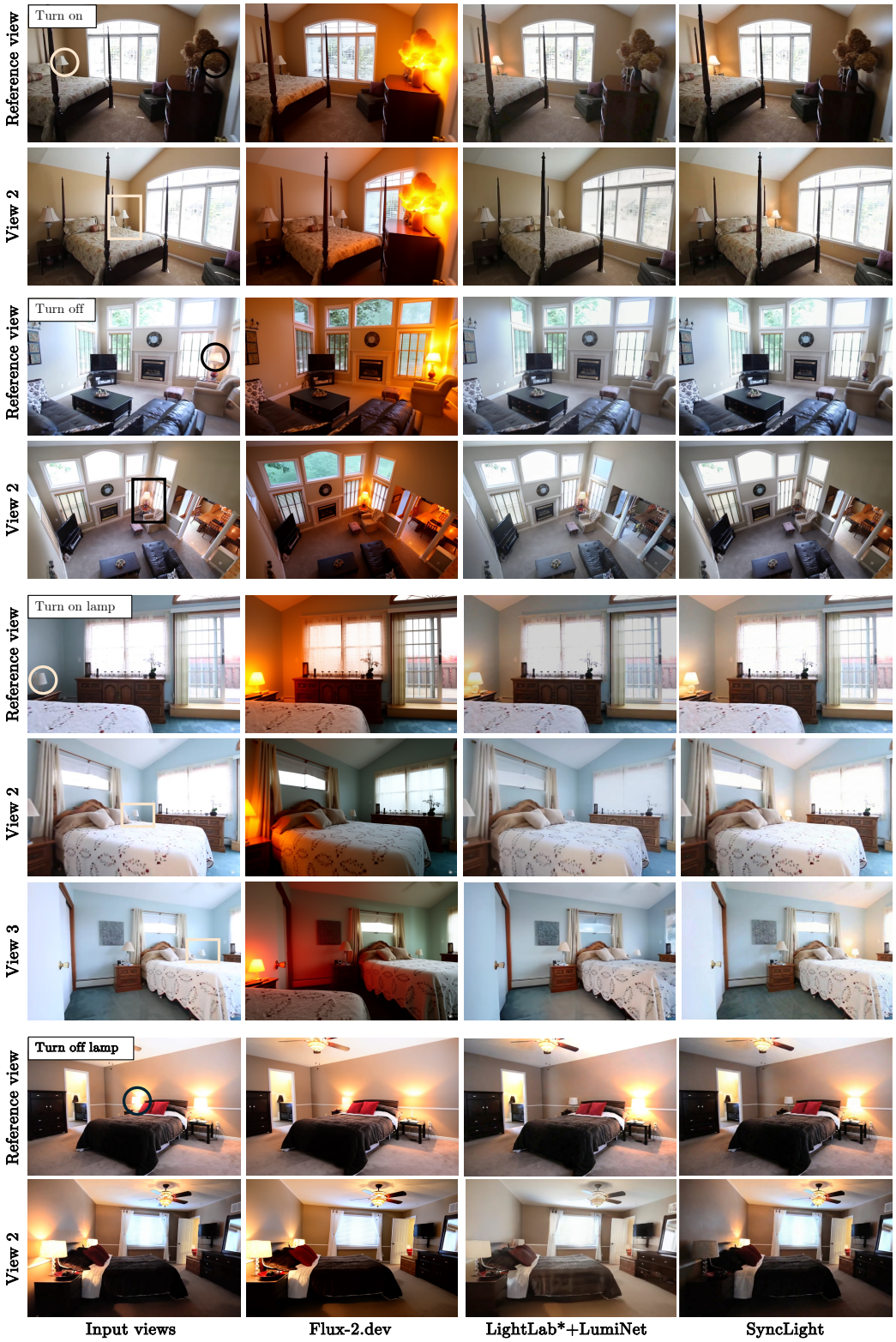


Figure 16: Additional results on the RealEstate10K dataset.

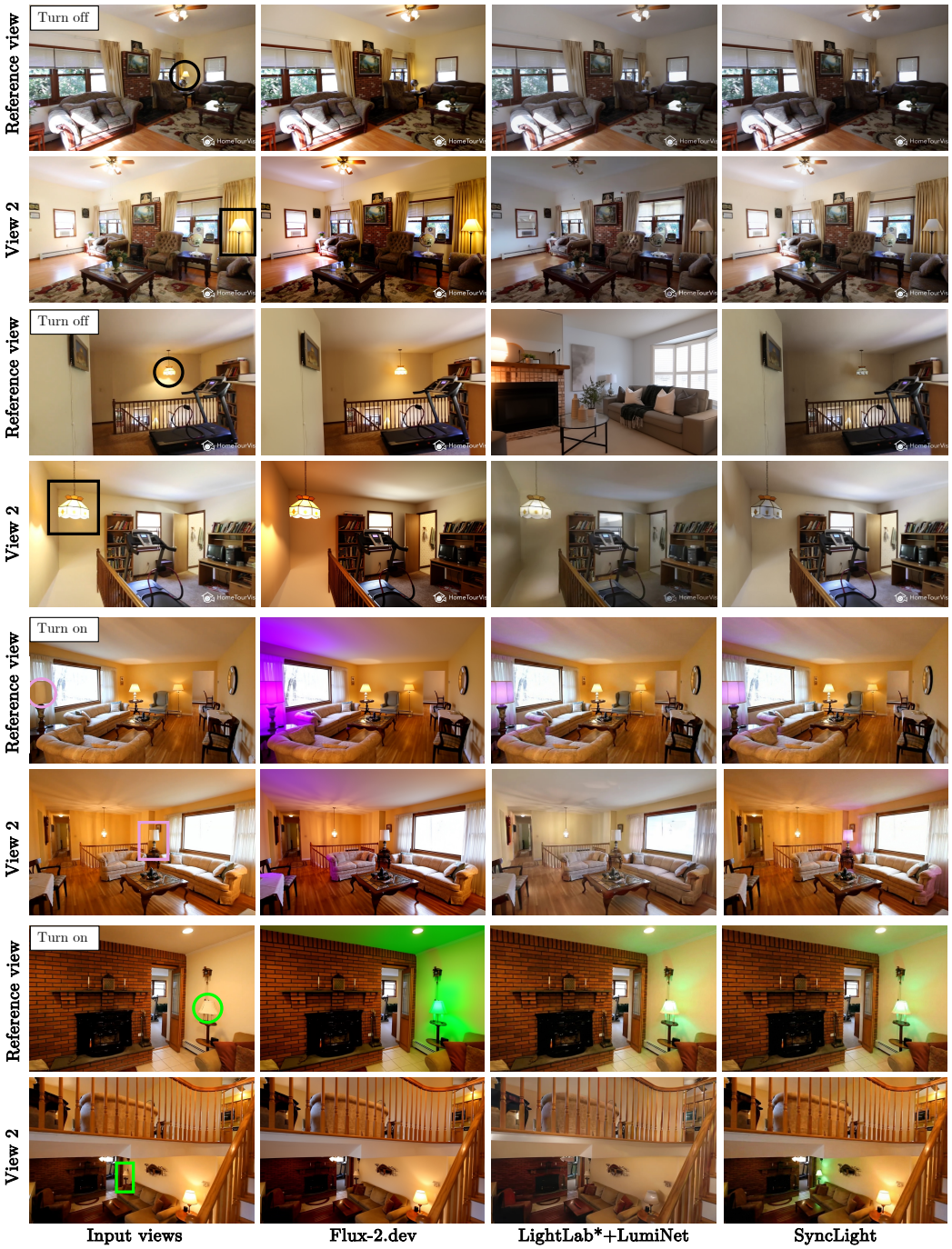


Figure 17: Additional results on the RealEstate10K dataset